FOIA MARKER

This is not a textual record. This is used as an administrative marker by the William J. Clinton Presidential Library Staff.

Collection/Record Group: Clinton Presidential Records

Subgroup/Office of Origin: Council on Environmental Quality

Series/Staff Member: Kathleen (Katie) McGinty

Subseries:

OA/ID Number: 2893

FolderID:

Folder Title:
Lindzen - Humidity Tests

Stack:	Row:	Section:	Shelf:	Position:
S	61	5	11	3

Richard S. Lindzen, Alfred P. Sloan Professor of Meteorology

Massachusetts Institute of Technology *(617) 253-2432*
Building 54, Room 1720 *fax (617) 964-3953*
Cambridge, Massachusetts 02139

January 20, 1993

Vice President Al Gore
Blair House
Washington, DC

Dear Vice President Gore:

I hesitate to impose on your time, but in view of our mutual interests, I thought that you might be interested in some possibilities for resolving our differences. None of the possibilities provide any occasion for financial gain for me or my research activities.

For a variety of reasons, the water vapor feedback cannot be measured locally. Essentially global averages are needed. Abraham Oort (at the Geophysical Fluid Dynamics Laboratory in Princeton University) has attempted such a study using standard radiosonde data. He analyzed the direct response of upper tropospheric water vapor to the global warming of the late 70's. I enclose a draft of some of his work. The decrease in upper level water vapor that he finds would, if correct, imply an equilibrium response to doubling CO_2 of less than 0.25°C. Although Oort's approach is viable in principle, there is, unfortunately, good reason to worry about the quality of the data. The point, simply, is that there have been changes in the sensors used on balloons to measure water vapor, and it is possible that the newer instruments are giving lower readings. It is also possible that the situation could be remedied by running a series of instrument intercomparisons over a full year at a variety of locations. This could lead to suitable recalibrations and consistent analyses of past data. In brief, it may be possible to resolve an important issue with data that is already available.

The next possibility is much more ambitious. Enclosed are two items:

1) A pair of papers explaining why routine satellite observation is likely to be of limited value; and

2) A white paper I prepared a couple of years ago on replacing current global balloon measurements (the primary data base for weather forecasting, etc.) with a network of unmanned high altitude aircraft.

The aircraft network would, among numerous other benefits, allow far more accurate measurement of water vapor. This is simply because the sensors, dropped from the aircraft, would not be contaminated by passage through the moist surface boundary layer.

For over thirty years, there has been an automatic identification of high technology with space. Phrased in this way, it may not be surprising that space based approaches to problems are increasingly antique and unimaginative. The proposed aircraft network is truly new and high tech. It also makes state of the art science far more accessible. Finally, the deployment of such a fleet of aircraft circling the earth would beautifully symbolize the end of the cold war.

I look forward to hearing your views on the above. Good luck in your new position.

Sincerely yours,

Richard S. Lindzen

Enclosures:

Oort
Lindzen & Fox-Rabinovitz
Fox-Rabinovitz & Lindzen
Unmanned Aircraft ....

11/30/1992

Observed humidity trends in the atmosphere

Abraham H. Oort

Geophysical Fluid Dynamics Laboratory/NOAA
Princeton University
Princeton, New Jersey 08542

- to appear in -

Proceedings of the 17th Annual Climate Diagnostics Workshop
held at the University of Oklahoma, Norman, OK on
October 19-23, 1992.

OBSERVED HUMIDITY TRENDS IN THE ATMOSPHERE

Abraham H. Oort

Geophysical Fluid Dynamics Laboratory/NOAA
Princeton University
Princeton, New Jersey 08542

Introduction: Water is one of the central elements in the earth's climate engine linking the atmosphere, oceans, cryosphere, land surfaces, and biosphere. In the atmosphere, water vapor strongly influences the radiation and energy budgets, and acts as an important greenhouse gas.

We will consider here two measures of the atmospheric moisture, namely the specific humidity q and the relative humidity $RH=q/q_s$, where q_s is the saturation specific humidity. Main emphasis will be on the upper air records for the 26-year period May 1963-Dec 1989 analyzed at GFDL based on twice daily observations from the global rawinsonde station network (Oort, 1983, NOAA Prof. Paper, 14).

The water vapor climatology is usually presented in terms of the specific humidity, as shown for example in the cross section in Fig. 1a. However, this diagram mainly reflects the structure of the temperature through the Clausius-Clapeyron equation, showing an exponential decrease of q with altitude, and a monotonic decrease of q with latitude. On the other hand, the cross section of relative humidity in Fig. 1b depicts more the atmospheric dynamics with, as expected, an equatorial maximum in

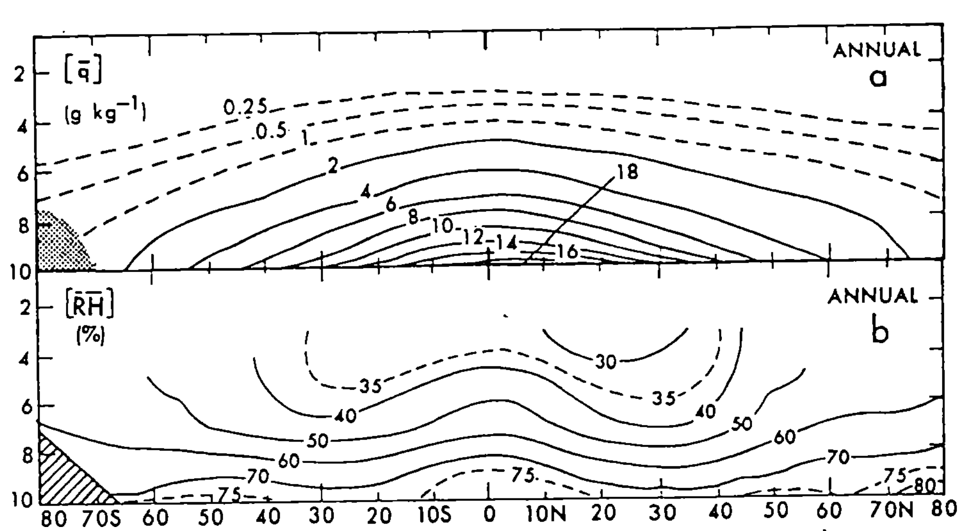

Fig. 1 Zonal-mean cross sections of (a) specific humidity q in g kg^{-1} and (b) relative humidity RH in % for annual mean conditions.

humidity in the rising branches of the tropical Hadley cells and subtropical minima in the sinking branches of the Hadley and Ferrel cells.

We may note that numerical weather prediction models as well as general circulation models (GCMs) have great difficulties to adequately represent the moisture distribution in the atmosphere. This is due to our lack of knowledge of how to parameterize the convective processes in the atmosphere and due to the resulting uncertainties in the vertical distribution of moisture.

The rawinsonde observations of moisture themselves are also subject to considerable uncertainties (much more than in the case of temperature) related to instrumental measurement difficulties at low temperatures and low pressures, the variety of instruments in use over the globe, and the different reporting practices that occasionally have changed during the period of record (e.g. Elliott and Gaffen, 1991, Bull. Amer. Meteor. Soc., 72). In spite of these obvious problems, we have accepted in the present study the station reports as true values. This may, to some extent, be justified because of the large-area and long-time averages considered here, which tend to reduce the errors. However, in certain situations systematic errors may remain and may affect some of our results, especially at low temperatures.

Time Series: Seasonal mean anomaly curves of specific humidity averaged over the two hemispheres are shown in Fig. 2 at various pressure levels. In both hemispheres, we find a clear upward trend of humidity in the lower troposphere, and a weaker downward trend in the upper troposphere. The level of no change seems to be located somewhat lower in the Southern Hemisphere (about 700 mb) than in the Northern Hemisphere (about 500 mb).

Comparing the q-curves with the corresponding curves for temperature in Fig. 3, we notice rising temperatures at all levels in the troposphere with the clearest rises between 850 and 500 mb. At the lower levels, the observed temperature and specific humidity variations seem to be consistent assuming a more or less steady relative humidity (within a few percent). There seems to be even a good correspondence between individual interannual peaks and valleys in q and T. However, the correspondence is not very good in the upper tropospheric levels, where the time series of relative humidity in Fig. 4 show, in fact, a strong downward trend, especially in the Southern Hemisphere.

Trends: We have calculated linear trends based on the annual mean station values and constructed zonal mean cross sections to show the vertical and latitudinal structure of the trends. The results given in Fig. 5 show that the rise in temperature (middle) and specific humidity (top) are strongest in the tropical troposphere (values of 0.2 (g kg^{-1})/10 yr and 0.2°C/10 yr are significant at the 95% confidence level). There seems to be

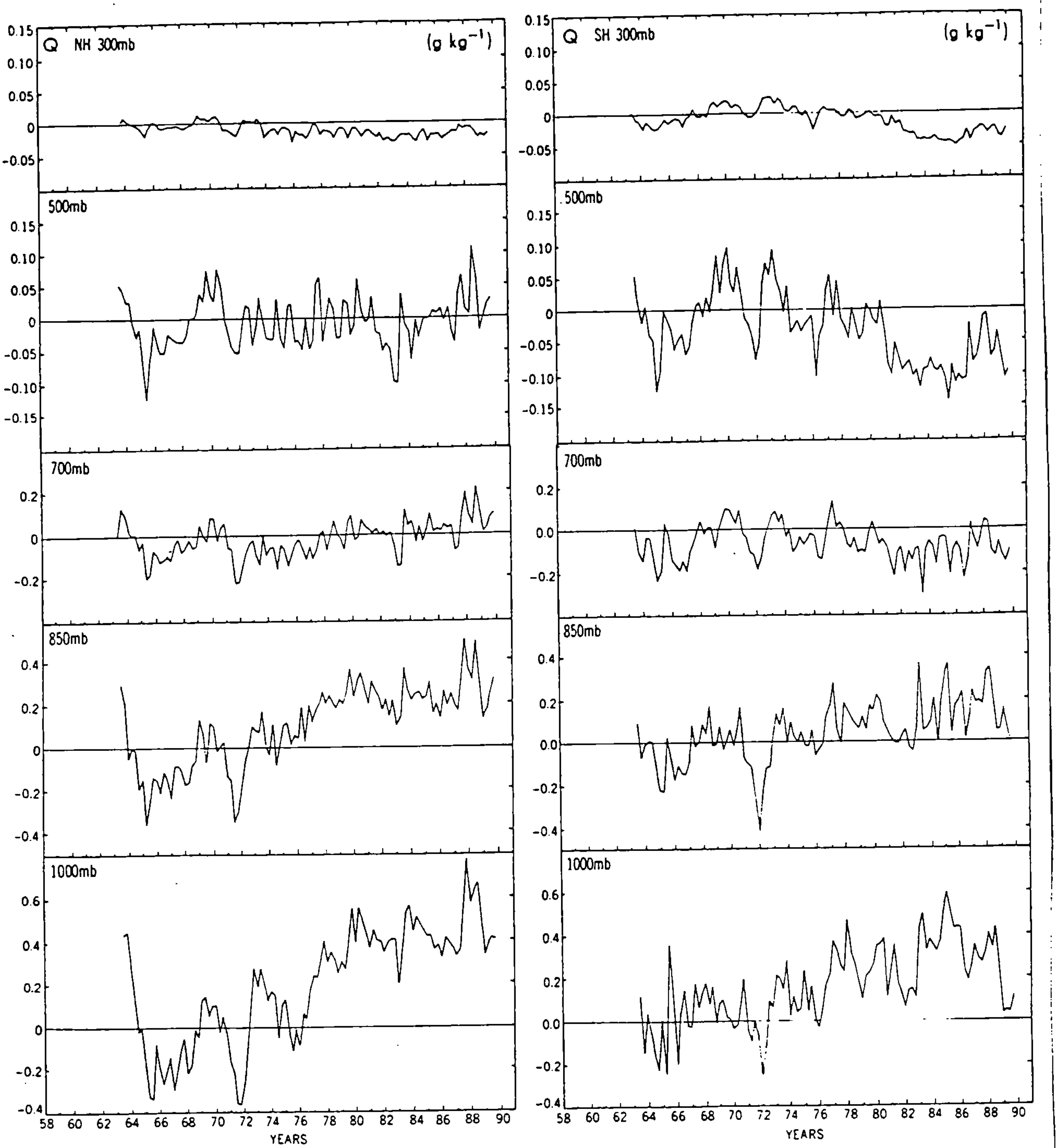

Fig. 2 Time series of the seasonal mean anomalies of specific humidity q in g kg^{-1} between June-August 1963 and September-November 1989 for the Northern (left) and Southern Hemisphere (right) at various pressure levels between the surface and 300 mb. These hemispheric mean values are based on objective global analyses made at GFDL using all available rawinsonde stations (ranging from about 600 stations in 1963 to about 800 stations in 1989).

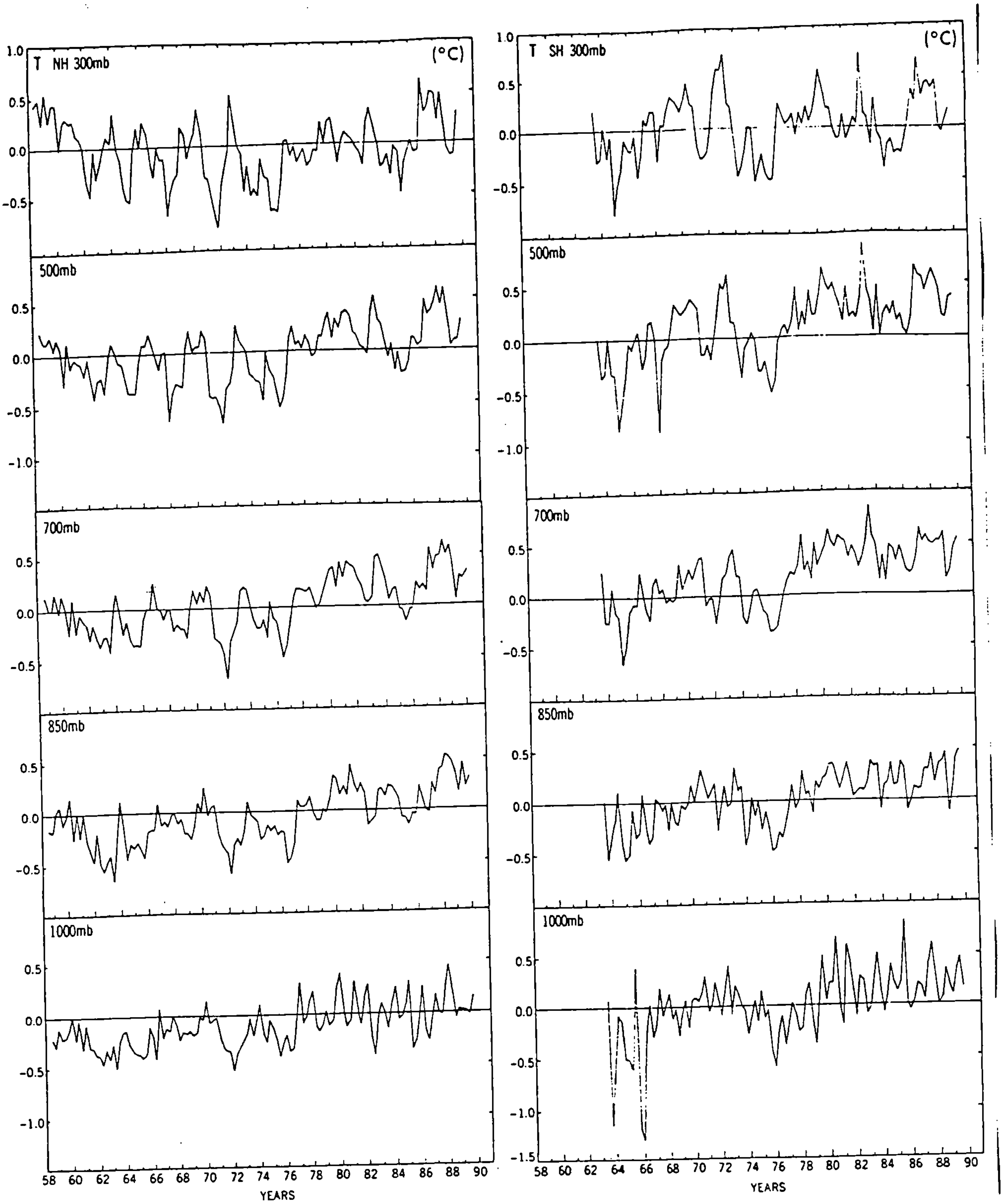

Fig. 3 Time series of the seasonal mean anomalies of temperature T in °C between June-August 1958 and September-November 1989 for the Northern (left) and Southern Hemisphere (right) at various pressure levels between the surface and 300 mb. Note that for the first five years only Northern Hemisphere values were analyzed because of the sparseness of data south of about 20°S (for more information on temperature trends, see Oort and Liu, 1993, J. Climate, 6, No. 1).

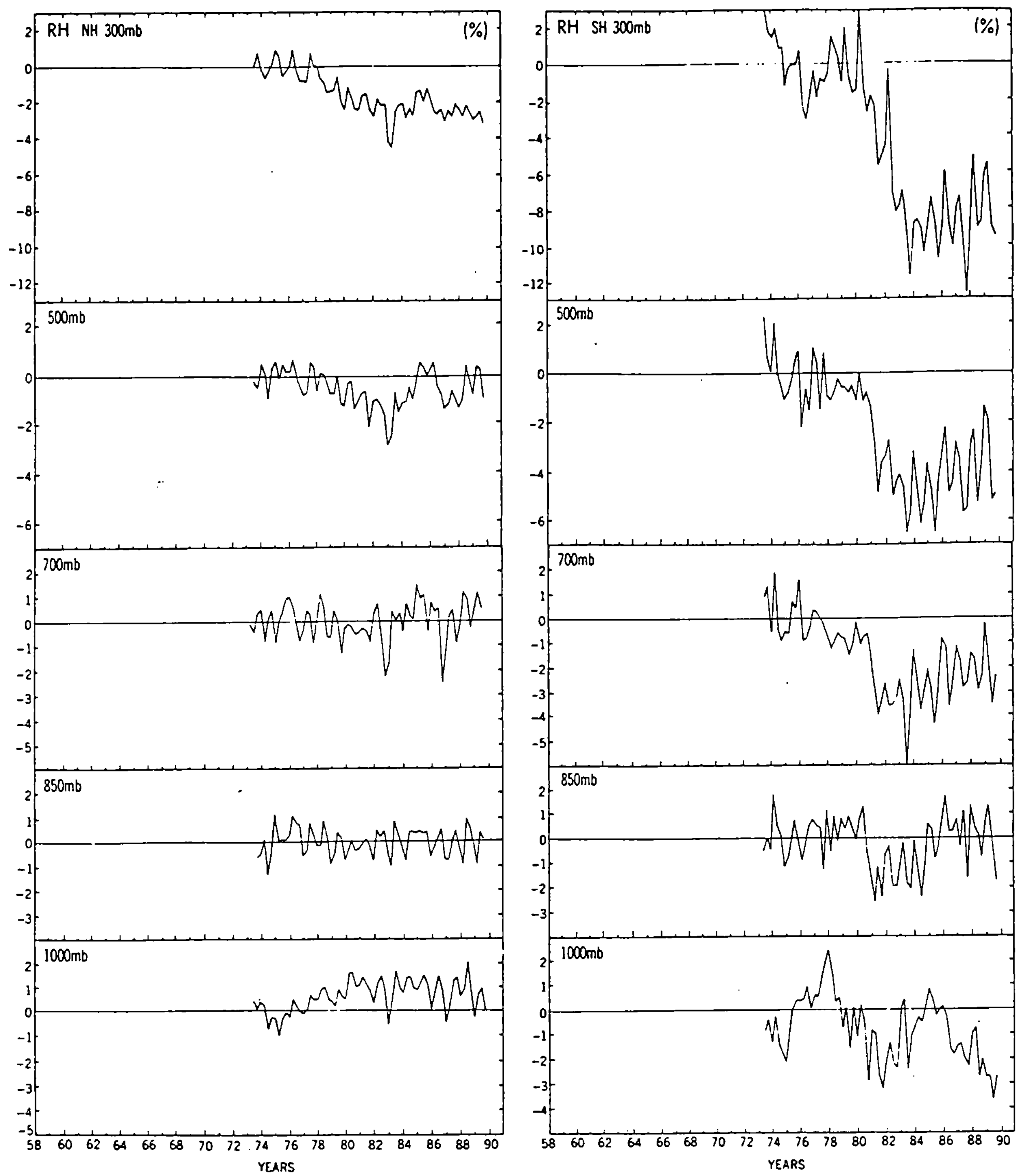

Fig. 4 Time series of the seasonal mean anomalies of relative humidity RH in % between June-August 1973 and September-November 1989 for the Northern (left) and Southern Hemisphere (right) at various pressure levels between the surface and 300 mb. Note that the relative humidity was analyzed only beginning May 1973 based on daily station reports.

some tendency for drying out in the subtropics above 700 mb (although not significant at the 95% level), and in the mid and high latitudes. This last feature is especially clear in the relative humidity where we find spectacular drops over -4%/10 yr (significant at the 95% level). We believe that these trends are

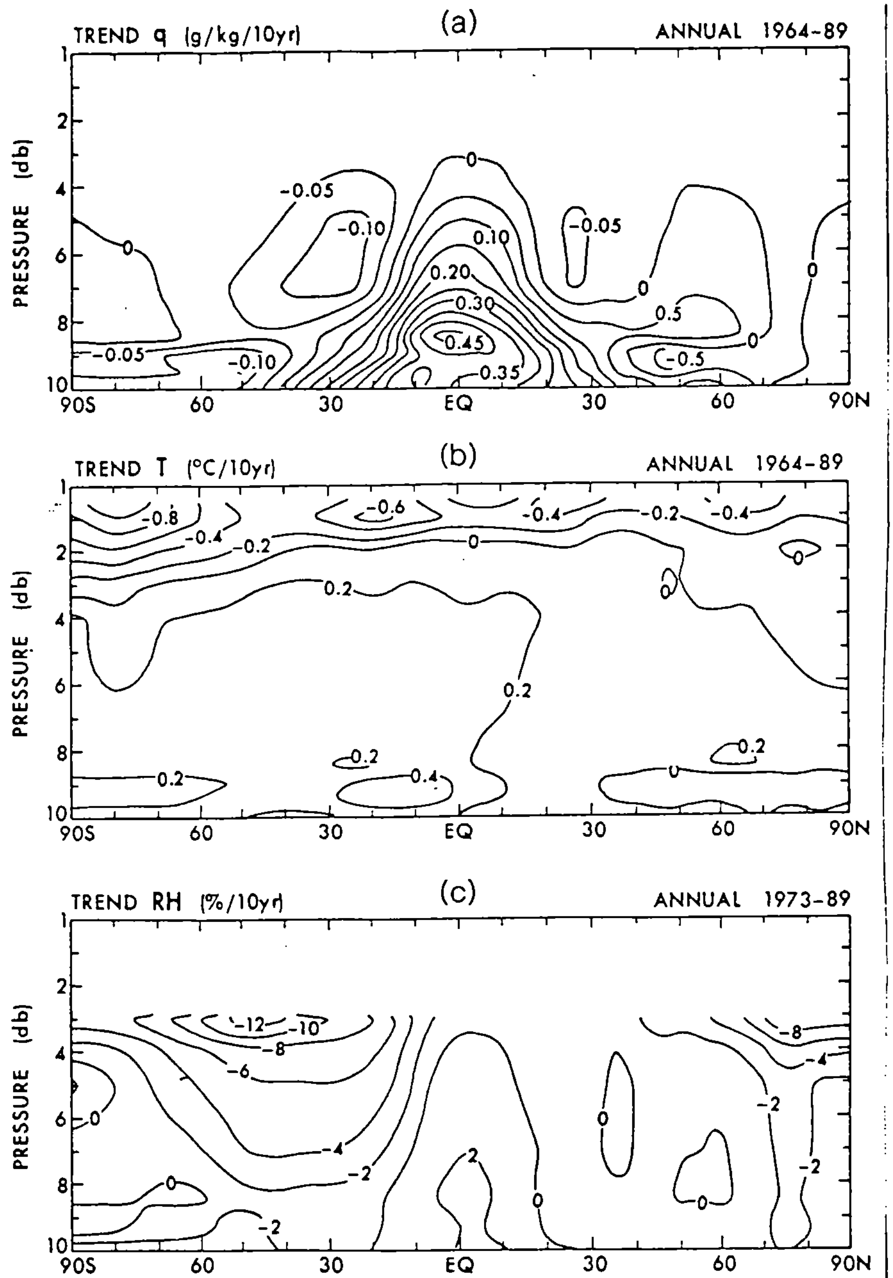

Fig. 5 Zonal mean cross sections for annual mean conditions of the linear trends in (a) specific humidity in units of (g kg^{-1})/10 yr, (b) temperature in °C/10 yr, and (c) relative humidity in %/10 yr. Note that these values are based on global analyses of the station trends at various pressure levels for the period January 1964-December 1989 in the case of q and T, and for the period January 1974-December 1989 in the case of RH.

of the correct sign, but that they are probably too strong because, in particular, above 500 mb the estimates of relative humidity tend to be less reliable due to the instrumental and reporting problems mentioned earlier. The resulting uncertainties will be investigated in later studies.

Finally, we show a global map of the trend in total annual precipitable water in Fig. 6. The map is dominated by areas of strong moistening up to 0.4 cm/10 yr over the equatorial regions of South America, Indonesia and the Central Pacific Ocean. Some weak areas of drying are found over Africa and in the midlatitudes. This global map is also very interesting since it resembles maps of the GCM expected increases associated with global greenhouse warming (T. Knutson, GFDL, private communication).

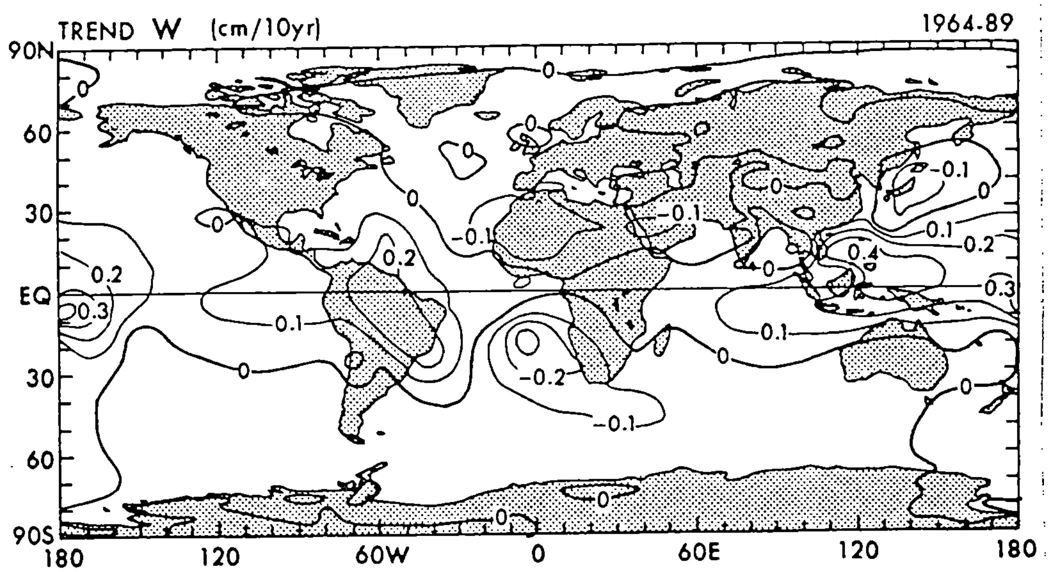

Fig. 6 Global distribution of the linear trend in annual-mean precipitable water W in the atmosphere in units of cm/10 yr for the 26-yr period January 1964 through December 1989.

<u>Conclusions</u>:

1. Specific humidity appears to have increased in the tropics during the last 25 years, with a maximum value of 0.45 g/kg/10 yr at 850 mb near the equator.

2. In mid and high latitudes there may have been slight decreases in specific humidity.

3. Changes in relative humidity appear to have been small (a few %/10 yr), except for the decreasing trend in mid and high latitudes. This trend may have been especially strong (greater than -4%/10 yr) above the 700 mb level.

Reprinted from MONTHLY WEATHER REVIEW, Vol. 117, No. 11, November 1989
American Meteorological Society

Consistent Vertical and Horizontal Resolution

RICHARD S. LINDZEN

Center for Meteorology and Physical Oceanography, Massachusetts Institute of Technology, Cambridge, Massachusetts

MICHAEL FOX-RABINOVITZ

Laboratory for Atmospheres, Goddard Space Flight Center, Greenbelt, Maryland

(Manuscript received 12 January 1989, in final form 9 June 1989)

ABSTRACT

Simple physical relations (namely, the Rossby ratio between vertical and horizontal scales in quasi-geostrophic flow and the dispersion relation for internal gravity waves) are used to estimate the vertical resolution consistent with a given horizontal resolution. Using these relations we find that virtually all large scale models and observing systems have inadequate vertical resolution. In models, the excess horizontal resolution can lead to increased model "noise" rather than improved accuracy. In observing systems, the finer horizontal scales can be severely misrepresented.

1. Introduction

We have long known that a given spatial resolution demands a minimum time resolution in order to avoid numerical instability (Courant et al. 1928). The mechanistic basis for this instability is reviewed in appendix A. Briefly, the instability arises when the spatial resolution defines modes whose time scale is too short to be resolved with the existing time steps.[1] *It should be emphasized that the striking implication of the CFL condition is that it calls for a time step that is usually much smaller than the time scale associated with the dominant spatial scale of the phenomena being described.* The point is that as long as we resolve the smaller scales for which the CFL condition may be violated, these scales will eventually be excited by nonlinearity or even roundoff error.

More recently, it has been noticed that a similar consistency requirement exists between vertical and horizontal resolution. It was noted by Hong and Lindzen (1976) that excessive horizontal resolution could resolve modes whose vertical wavelength might be too small to be resolved with the existing vertical resolution, and that this situation could lead to spatial instability (Lindzen 1970). When the radiation condition is used, this can actually lead to spurious amplitude growth with height; when there is a lid, the manifestation is more complicated. When there are so few levels that spurious growth can't manifest itself, one simply obtains incorrect solutions (Lindzen et al. 1968). *Here too, the vertical resolution may be adequate for the horizontal scales one is physically concerned with. Smaller scales, however, are inevitably generated in the course of integration.* Despite this awareness, little evidence in the literature shows that any serious attempt is being made to achieve any consistency between horizontal and vertical resolution in general circulation models, in models for numerical weather prediction, or even in so-called mechanistic models (for stationary waves, sudden warmings, etc.). This is despite the fact that the problem was early recognized by Charney (1949).

The purpose of the present note is to develop criteria for such consistency and to examine current models in the light of these criteria. The criteria developed also apply to the resolution of observing systems, and we shall examine this as well.

2. Consistency relation

In general, the atmosphere supports a variety of physical wave mechanisms, and it is difficult, therefore, to uniquely establish a consistent relation between horizontal and vertical resolution. We shall separately consider the quasi-geostrophic regime and the scaling appropriate to gravity waves.

a. Quasi-geostrophic flows

If one restricts oneself to waves which are quasi-geostrophic, then a relation between horizontal and vertical

Corresponding author address: Dr. Richard S. Lindzen, Center for Meteorology & Physical Oceanography, M.I.T., 77 Massachusetts Avenue, Cambridge, MA 02138.

[1] To be sure, one can avoid explicit numerical instability by using semi-implicit time differencing; however, failure to satisfy the CFL condition is inevitably accompanied by gross inaccuracy even in the absence of numerical instability.

On Replacing the Global Radiosonde Network with a Fleet of Remotely Controlled Pilotless Aircraft with Dropsondes.

R.S. Lindzen
54-1720, M.I.T.
Cambridge, MA 02139
(617-253-2432)

1. Preliminary Remarks.

Present Radiosonde Network

The present network consists in about 450 irregularly spaced stations with minimal coverage over the oceans and in the Southern Hemisphere. At most stations, soundings are made only twice a day, though at some stations soundings are made four times a day. Soundings are nominally made simultaneously at all stations (i.e., at the same Universal Time).

Current Satellite Radiance Data

The poor vertical resolution of temperature retrievals from satellite infrared radiance limits effective horizontal resolution to over 1200 km. On the accompanying figures results from the NASA GLA assimilation scheme show that verification of the satellite data does not begin to deteriorate until the initial data is smoothed over 4-6 gridpoints (grid intervals are 250 km). Such data represents coverage worse than that provided by radiosondes over much of the Northern Hemisphere. It will be impossible to achieve an adequate monitoring capability with such data.

Proposed Pilotless Aircraft Network

The proposed network will provide data superior to current radiosonde data at 3000 regularly spaced observation points with four soundings per day at each point. The soundings would be provided by dropsondes which would provide measurements of wind, temperature, and humidity. As noted later, the planes could also carry passive radiometers.

2. Simple-minded Flight Strategy

Aircraft fly at ground speed of 300 km/hr. At each latitude circle (at 5 degree intervals), launch a plane every 6 hours (to yield four soundings per day at each point). The number of planes needed at each latitude is essentially the time it would take for a plane to circumnavigate the globe at that latitude divided by 6. (See accompanying table.) The estimated number of planes is slightly higher than the figure used above. Dropsondes would be ejected hourly from each plane.

3. Estimated costs

Aircraft (Aurora Perseus II's)

Number[1]	500
Annual cost[2]	$250,000
Additional hourly cost[3]	$250
Cost per dropsonde[4]	$200

Annual cost = 500 x 250,000 + 500 x 24 x 365 x (250 + 200) = $2,096,000,000.

Current Radiosonde Network

Annual cost/ station	$400,000
Cost/sonde	$50

Annual cost = 450 x 400,000 + 450 x 3 x 365 x 50 = $204,637,500.

Note that the aircraft system costs what a comparably large radiosonde network would cost, but it would be impossible to set up radiosonde stations over the oceans. Moreover, one may plausibly expect significant reductions in the estimated cost of the aircraft network to arise from economies of scale, and from more efficient flight track strategies.

4. Trial Study

A reasonable trial of the above system might consist of 18 aircraft flying rectangular paths of size 500 km north-south and 4800 km east-west. Such a system could provide the above described resolution for a region west of the Pacific Coast of North America extending 3000 km in the north-south direction and 4800 km in the east-west direction. The impact of such data on numerical weather forcasts should be readily assessed. Such a study could be conducted for a month at a cost of about $20,000,000.

5. Notes

The aircraft system offers immense flexibility *vis a vis* both the conventional radiosonde network and a satellite system. Planes may be reinstrumented and paths alterred on short notice. Passive radiometry can be done from the planes with the advantage that one can independently look up and down. Planes may moreover include vertical sections in their paths to directly sound sections of the atmosphere. Extra planes would be readily available for special purposes. Even the routine resolution provided by the proposed network would be comparable to that provided during some intensive field studies.

Psychologically, the airplane network offers a new, more human image for big science. Children playing with remotely controlled model airplanes would have a meaningful connection to the aircraft weather and climate monitoring system. More advanced students would have convenient access to and influence on the aircraft data and its acquisition.

It should be added that the proposed aircraft network is truly high tech. Its development depends critically on recent developments in material science, microelectronics, etc.

Endnotes

1. Based on non-optimized track. See section 3.

2. No economies of scale assumed.

3. No economies of scale assumed.

4. Current price. However, we expect that for large quantities, the price can be reduced to $100.

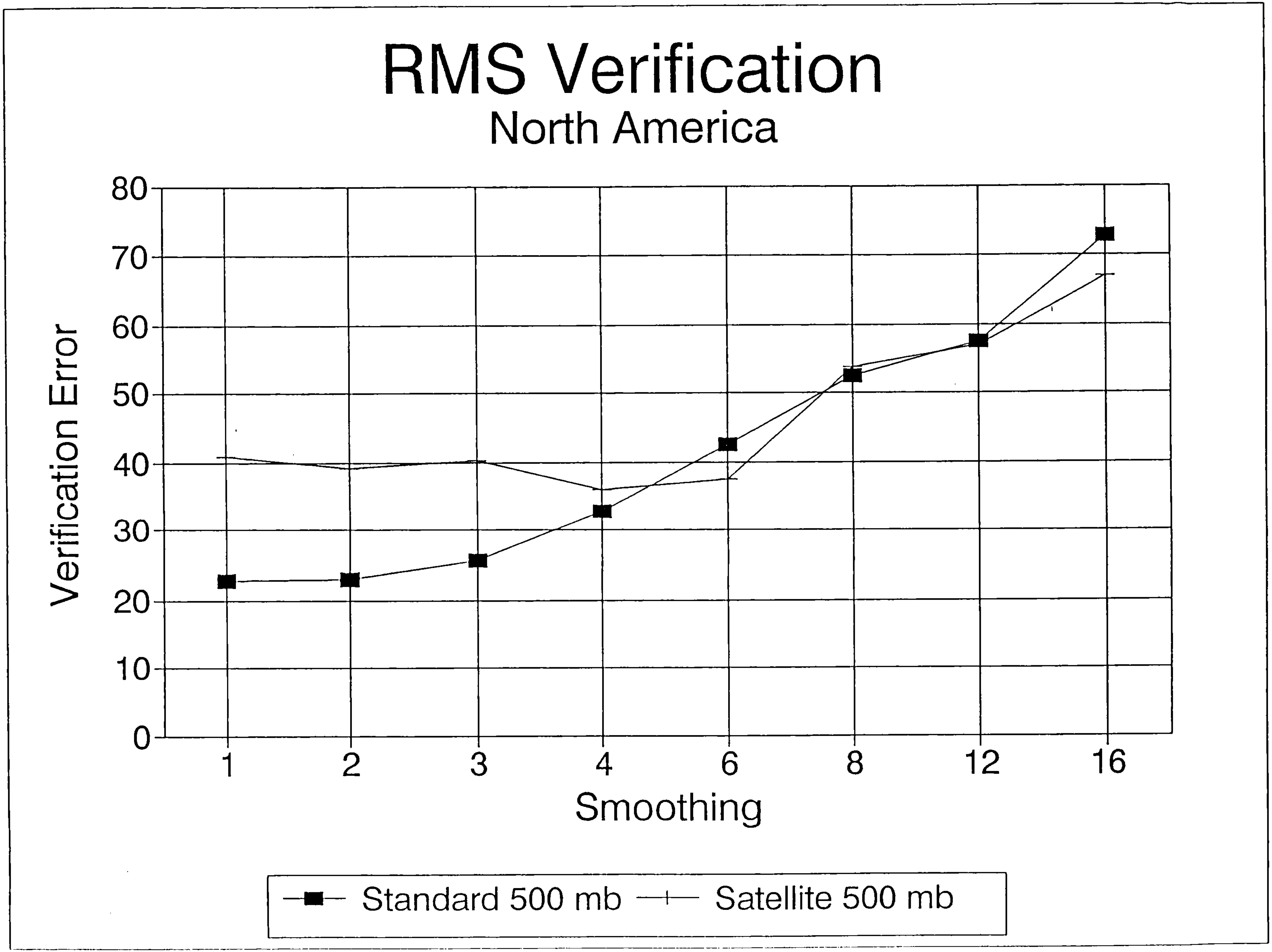
RMS Verification
North America
Verification Error
80
70
60
50
40
30
20
10
0
1
2
3
4
6
8
12
16
Smoothing
Standard 500 mb
Satellite 500 mb

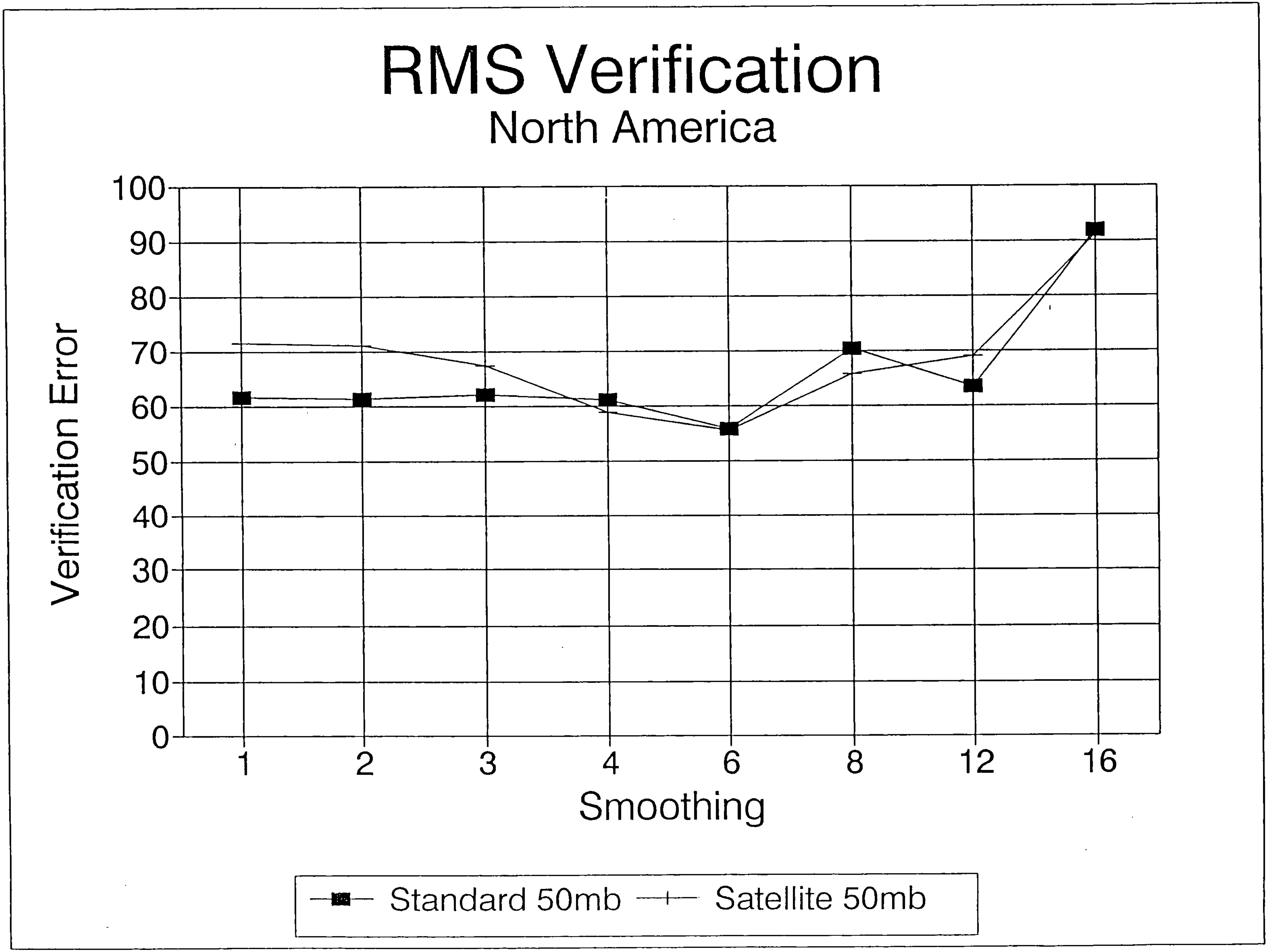
RMS Verification
North America
100
90
80
70
60
50
40
30
20
10
0
Verification Error
1
2
3
4
6
8
12
16
Smoothing
Standard 50mb
Satellite 50mb

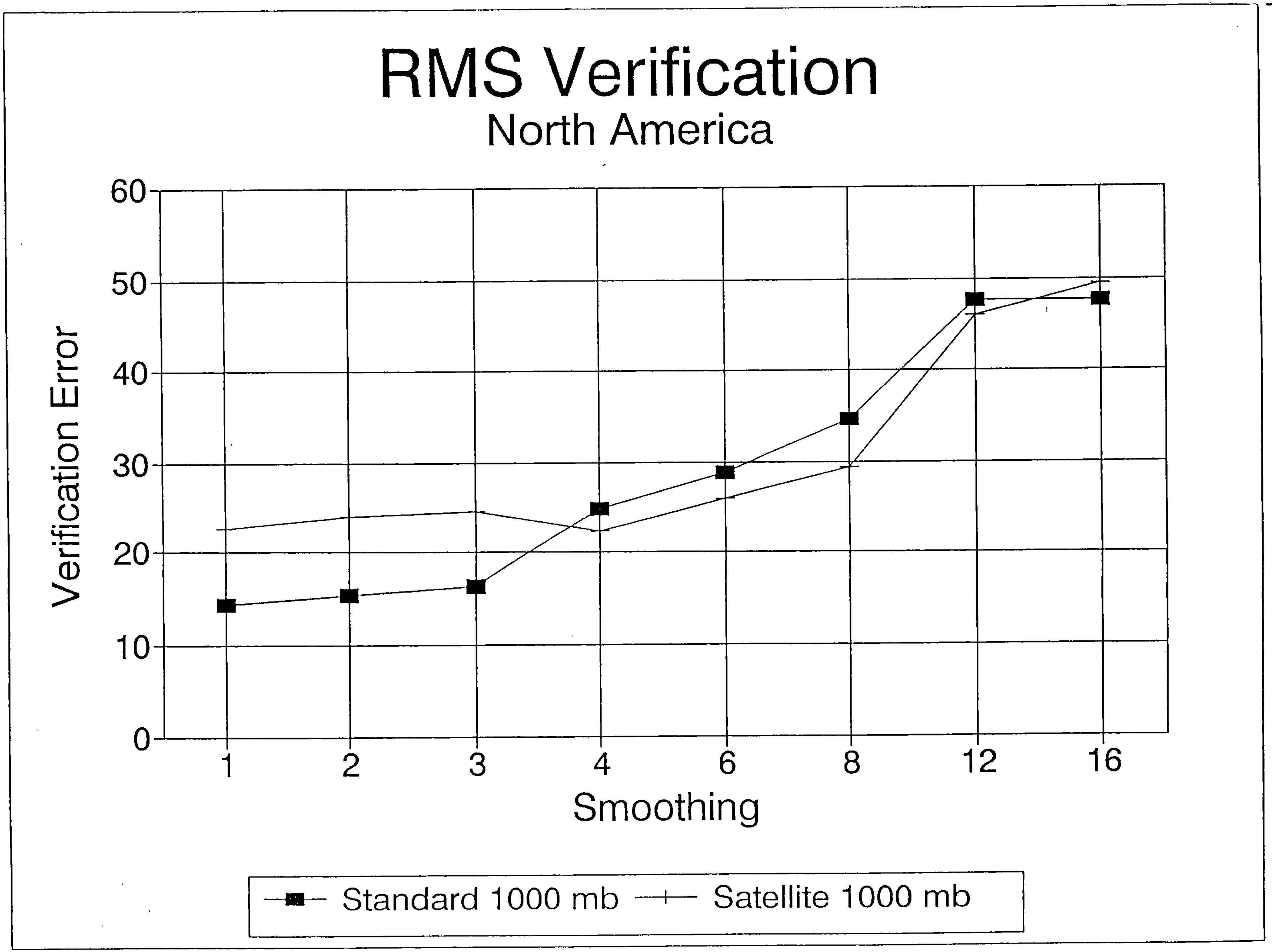

RMS Verification
North America
Verification Error
60
50
40
30
20
10
0
1
2
3
4
6
8
12
16
Smoothing
Standard 1000 mb
Satellite 1000 mb

Planes needed for 5 deg meridional and 300 km zonal coverage

(At each latitude circle, number of planes =
Circumference/ Ground Speed/ 6 hours)

Latitude (degrees)	Circumference (kilometers)	Time at 300km/hr (hours)	Number of planes
0	40212	134	22
5	40059	134	22
10	39601	132	22
15	38842	129	22
20	37787	126	21
25	36445	121	20
30	34825	116	19
35	32940	110	18
40	30804	103	17
45	28434	95	16
50	25848	86	14
55	23065	77	13
60	20106	67	11
65	16994	57	9
70	13753	46	8
75	10408	35	6
80	6983	23	4
85	3505	12	2
90	0	0	0
	Total Number of planes		534

Aurora

March 13, 1991

Memorandum to: Jim Anderson

From: John

Subject: Annual costs of large-scale dropsonde network

This is a quick summary of the annual costs of a large dropwindsonde network. I have assumed:

• The Perseus B aircraft, cruising at 18 km at a speed of ~160 knots. The aircraft can cover over 6000 nm in a single 40-hour flight with a 200 kg payload. The direct operating cost shown includes all amortization, O&M, and personnel costs.

• A modified NCAR lightweight sonde weighs about 250 gram. Thus for 100 kg we could carry up to 400 sondes, still leaving 100 kg for other instruments such as data receiver/processor and satellite relay.

• Typical routes might include:

Alaska-Hawaii	2231 nm
Miami-Gibraltar	4000 nm
Bermuda-Iceland-Azores	6000 nm

Obviously, only a very small number of stations are needed to provide near-global coverage. I assumed that five basic routes would be laid out, with one flight per day launched over each route (note that on long routes, several flights are thus in progress at any one time).

The big driver is dropsonde cost. Current rawindsondes cost ~$50 each for basic sondes w/o radionav capability. NCAR sondes are presently $200-$400 each, but made by hand in very small quantities. A GPS front end receiver is currently about $800 but falling rapidly. Aurora has already held initial discussions with several rawindsonde manufacturers about producing a GPS-dropwindsonde. We feel the $200/sonde number is a reasonable target for the quantities envisioned here.

AURORA
FLIGHT SCIENCES CORPORATION
3107 COLVIN ST. • ALEXANDRIA, VIRGINIA 22314 U.S.A.
(703) 823-0497 • FAX (703) 751-6947

	A	B	C	D
4	Assumptions:			
5	Aircraft ($/hr)	520		
6	Mission length (hrs)	40		
7	Flights per day	1		
8	Days per year	365		
9	# Routes	5		
10				
11	Results:			
12	Cost per flight:	$20,800		
13	Flights per year:	1,825		
14	Cost per year:	$37,960,000		
15				
16	**ANNUAL COST**	Sonde unit cost		
17	Sonde dispensing rate (per hour)	$50	$200	$800
18	1	$41,610,000	$52,560,000	$96,360,000
19	5	$56,210,000	$110,960,000	$329,960,000
20	10	$74,460,000	$183,960,000	$621,960,000

Aurora could have a full operational demonstration within 18 months of go-ahead (and probably much sooner). The total cost including engine development, first batch of 2 aircraft, satellite data link, and sondes would be about $5 million.

AURORA
FLIGHT SCIENCES CORPORATION
3107 COLVIN ST. • ALEXANDRIA, VIRGINIA 22314 U.S.A.
(703) 823-0497 • FAX (703) 751-6947

Perseus B

PHYSICAL CHARACTERISTICS	
Span	17.9m
Wing Area	18.0m
Empty Weight	254kg
Gross Weight	696kg

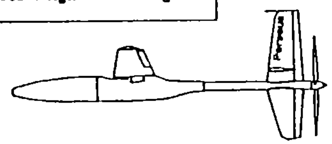

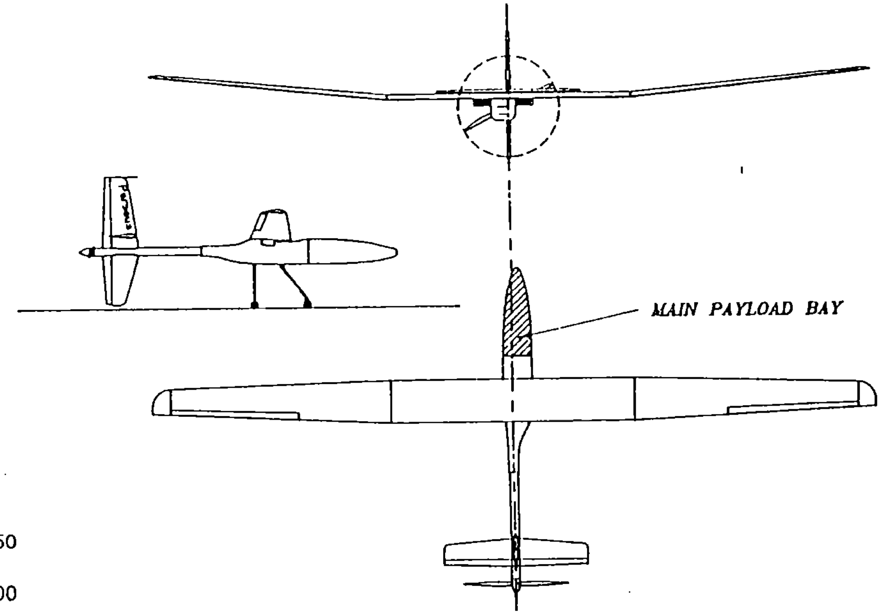

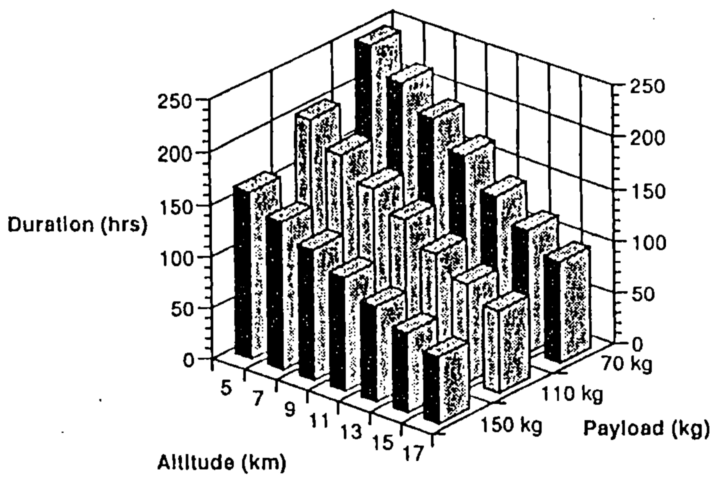

- tooling and control system adapted from Perseus A
- turbocharged IC engine
- gasoline as fuel
- retractable landing gear for operation at standard airports
- payloads up to 150 kg

Cost comparison of high-altitude platforms

	Perseus A	Perseus B	Theseus	ER-2	Gulfstream IV	Condor
GTOW (kg)	399	1500	1600	18120	33340	7112
Empty wt (kg)	245	600	850	8100	19252	1564
Altitude (km)	25	18	30	20	13.7	20
Payload (kg)	50	150	220	900	1900	650
Range (km)	500		5000	8100	9450	22000
Duration (hr)	6	36	10	8	10	42
Power (HP or lbs thrust)	30	23	160	26500	28000	360
Purchase cost ($)	$750,000	$750,000	$2,000,000	$20,000,000	$25,000,000	$50,000,000
Engine cost ($)	$150,000	$35,000	$250,000	$8,000,000	$8,000,000	$5,000,000
Fuel cost ($/lb)	$5.00	$0.30	$5.00	$0.20	$0.20	$0.30
Lifetime (hrs)	600	6000	9000	30000	20000	12000
Loss Rate (1:x ops)	100	500	1000	5000	5000	1000
Ave flight (hrs)	6	12	9	6	4	12
Utilization (hrs/yr)	300	1000	600	300	300	1000
Support org (# people)	10	10	20	50	5	50
Cost ($/person/yr)	72000	72000	72000	125000	125000	125000
# A/C per support unit	3	3	3	3	1	1
COSTS ($/flt-hr)						
Crew	$63	$63	$63	$65	$130	$64
Fuel	$191	$41	$650	$671	$1,345	$270
Insurance	$50	$15	$67	$1,333	$1,667	$1,000
Maintenance	$40	$35	$47	$419	$531	$362
• A/C labor	$15	$15	$16	$71	$144	$29
• A/C material	$3	$3	$8	$82	$116	$180
• Engine labor	$18	$17	$17	$65	$71	$27
• Engine material	$4	$1	$6	$200	$200	$125
Subtotal, DOC:	**$344**	**$155**	**$827**	**$2,488**	**$3,673**	**$1,696**
Depreciation	$1,250	$125	$222	$667	$1,250	$4,167
Total, DOC	**$1,594**	**$280**	**$1,050**	**$3,155**	**$4,923**	**$5,862**
IOC	$800	$240	$800	$6,944	$2,083	$6,250
Total Costs, $/hr	**$2,394**	**$520**	**$1,850**	**$10,099**	**$7,006**	**$12,112**

All estimates made using ATA "Standard Method for Estimating DOC"

Aurora

Perseus as a dropwindsonde deployment platform

- Vertical profiles of T, P, RH are essential for:
  - initializing forecast models
  - resolving issues of tropical water vapor budgets
  - studying and tracking severe storms
- With 100 lightweight dropwindsondes and a cruise altitude of 60,000 ft, *Perseus B* has a range of >7000 nm

Dropwindsonde specifications

mass	250 gm
dimensions	8.25 cm x 41 cm
descent rate	20 m/s at 12 km 9 m/s at sea level
transmitter power	1 W
temperature sensor	40 mil bead thermistor
humidity sensor	carbon with heated substrate
pressure sensor	piezo-resistive silicon
microprocessor	Motorola MC68HC11A8FN
navigation	LORAN

Instruments for hurricane reconnaissance mission

measurement	instrument	weight [kg]
temperature, pressure, relative humidity	dropwindsondes (120)	30
	dispenser	10
temperature, pressure	Meteorological Measurement System	5
data handling		35
total		80

Aurora

Cruise performance of Perseus B (as of 5 March 1991)

1000 kg take-off weight, 50 kW installed power

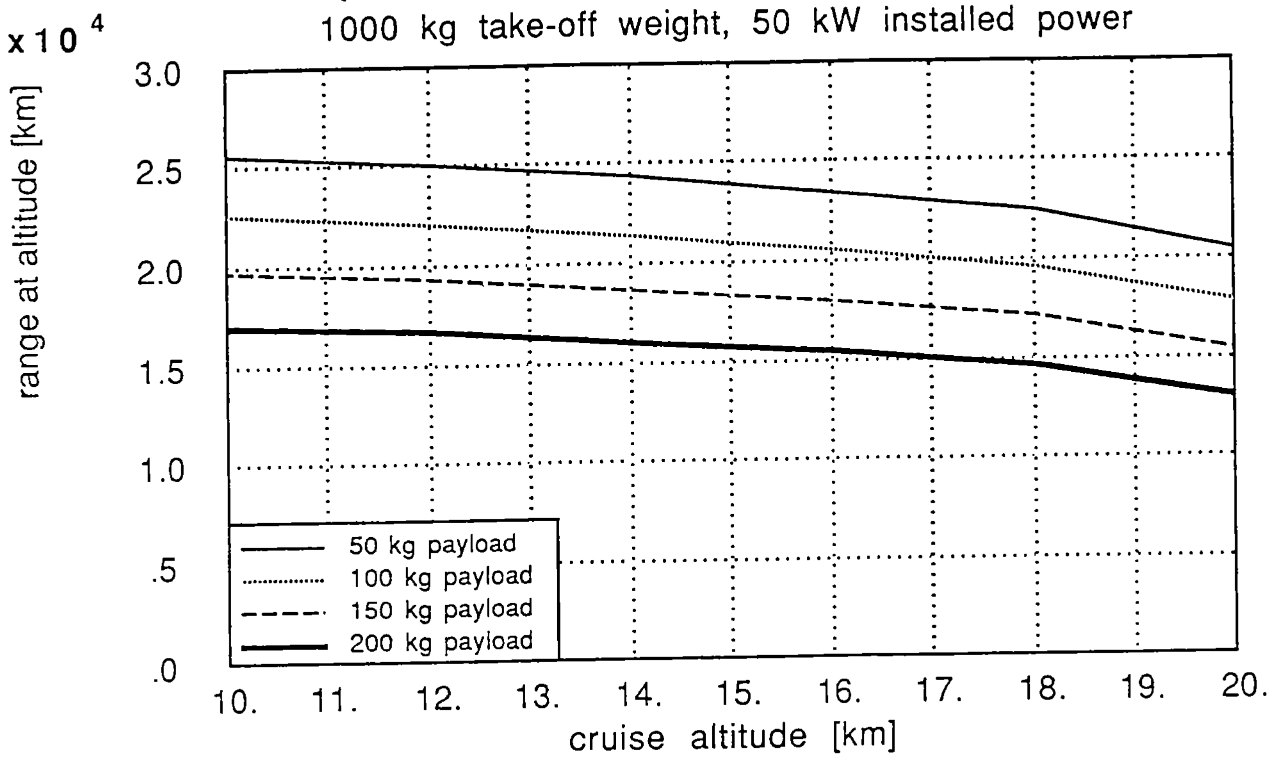

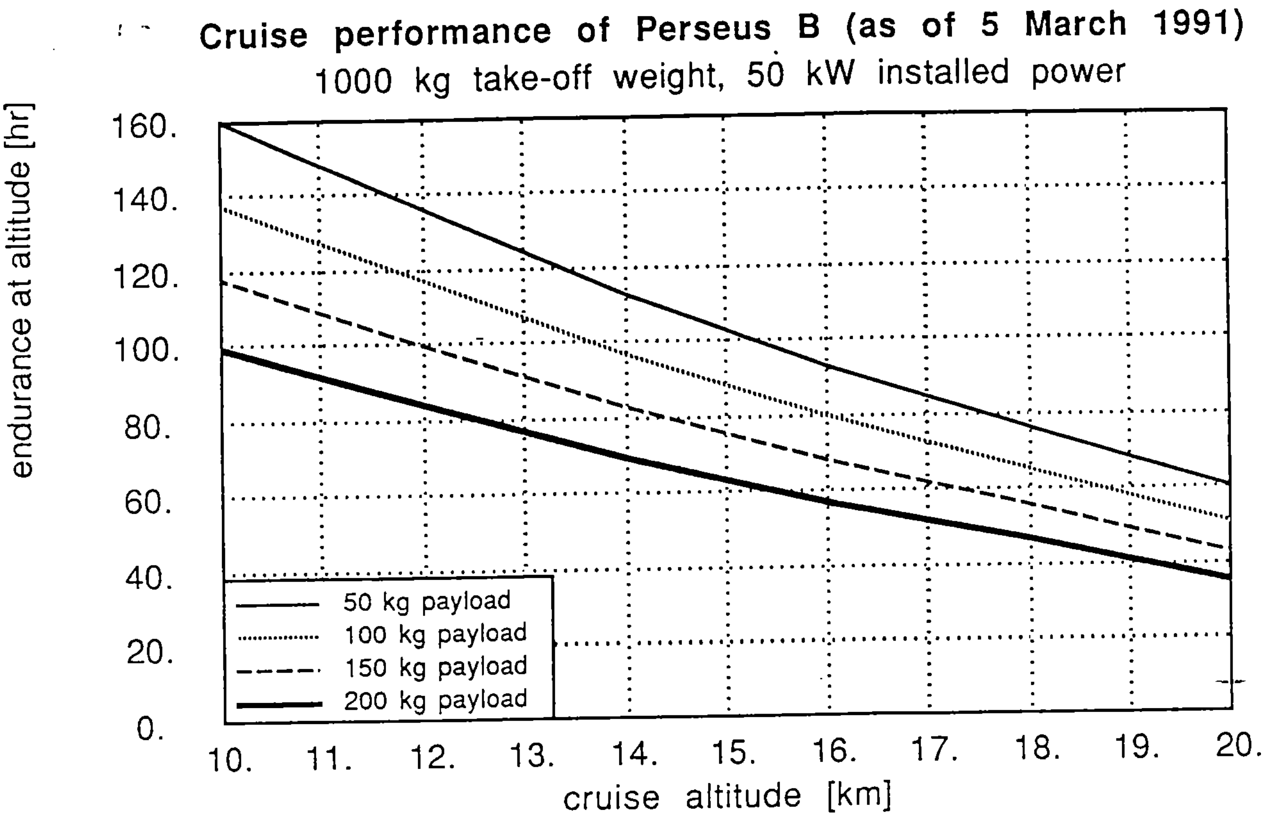
Cruise performance of Perseus B (as of 5 March 1991)
1000 kg take-off weight, 50 kW installed power
endurance at altitude [hr]
160.
140.
120.
100.
80.
60.
40.
20.
0.
10.
11.
12.
13.
14.
15.
16.
17.
18.
19.
20.
cruise altitude [km]
50 kg payload
100 kg payload
150 kg payload
200 kg payload

40 kg/hr

NUMERICAL EXPERIMENTS ON CONSISTENT HORIZONTAL AND VERTICAL RESOLUTION FOR ATMOSPHERIC MODELS AND OBSERVING SYSTEMS

Michael S. Fox-Rabinovitz[1]

Laboratory for Atmospheres

NASA/Goddard Space Flight Center

Greenbelt, MD 20771, USA

and

Richard S. Lindzen

Center for Meteorology and Physical Oceanography

Massachusetts Institute of Technology

Cambridge, MA 02139, USA

(Revised version submitted to Monthly Weather Review)

April 1992

[1] Universities Space Research Association

Corresponding author address: Dr. M. S. Fox-Rabinovitz, Code 910.3, Laboratory for Atmospheres, NASA/Goddard Space Flight Center, Greenbelt, MD 20771

ABSTRACT

Simple numerical experiments are performed in order to determine the effects of inconsistent combinations of horizontal and vertical resolution in both atmospheric models and observing systems. In both cases, we find that inconsistent spatial resolution is associated with enhanced noise generation.

A rather fine horizontal resolution in a satellite data observing system seems to be excessive when combined with the usually available relatively coarse vertical resolution. Using different strength horizontal filters, adjusted in such a way as to render the effective horizontal resolution more consistent with vertical resolution for the observing system, may result in improvement of the analysis accuracy. However, the increase of vertical resolution for a satellite data observing system is desirable. For the conventional data observing system with better vertically resolved data, the results are different in that little or no horizontal filtering is needed to make spatial resolution more consistent for the system.

The obtained experimental estimates of consistent vertical and effective horizontal resolution are in a general agreement with consistent resolution estimates previously derived theoretically by the authors.

1. INTRODUCTION

Along with improvements of initial data quality, numerical schemes, diabatic parameterization methods, and availability of more powerful computer systems, the gradual increase of horizontal and vertical resolution was one of the most important and straightforward components of the substantial improvement, in terms of the increased accuracy and practical reliability, of NWP models and GCMs during the last two decades.

Some currently used operational forecast or experimental models have fine and very fine horizontal resolution of the order of a few to several tens of kilometers for hurricane and mesoscale models, 50-150 km for regional, and 60-300 km for global models and GCMs. At the same time, these models usually have relatively limited levels in the vertical in the troposphere, and even poorer vertical resolution in the stratosphere. The vast majority of currently used NWP models and GCMs, even those with fine and very fine horizontal resolution have no more than 6-19 levels for the whole tropospheric and lower stratospheric vertical domain of integration. Note that recently some leading modeling groups are considering the possibility of increasing the model vertical resolution. An example is the new 31 level ECMWF model (Simmons 1991).

The same is true for current observing systems which have vertical resolution often even poorer than the aforementioned model resolution.

The discussion of consistent spatial resolution for numerical models and observing systems is presented in Lindzen and Fox-Rabinovitz (1989), hereafter referred to as LF. This paper contains some approximate estimates of consistent horizontal and vertical resolution for quasi-geostrophic, and gravity wave processes. It is worth emphasizing that even according to some of the most moderate estimates, the vertical resolution needed for describing quasi-geostrophic processes in middle latitudes should be increased (sometimes significantly) in order to be consistent with horizontal model resolution used by many models.

As recently noted by Persson and Warner (1991), inconsistent resolution can be shown to produce spurious gravity waves. This is broadly consistent with the present finding of increased "noisiness."

There are three different types of spatial resolutions related to atmospheric models and observing systems, namely, physical, computational, and observational resolutions. The last may be defined, for example, as a mean distance in the horizontal and in the vertical between observation locations. Such an observational resolution measure may be specified for particular regions.

Computational requirements on spatial model resolution allow us to keep a truncation error, or approximation accuracy within some reasonable range. It should guarantee, for example, that all physical scales resolved by a model are adequately represented by an appropriate number of gridpoints, or in other words, realistically described by a discretized system with a guaranteed approximation accuracy. The computational resolution usually imposes the strongest requirements on the number of gridpoints needed to represent the considered scales adequately.

The physically consistent resolution requirements, which will be discussed in this note, have to be derived from the basic properties of the atmospheric processes, and have to reflect, or correspond to their nature. The requirements of this kind on physically consistent horizontal and vertical resolution for large scale atmospheric models and observing systems are based on consideration of quasi-geostrophic flows, tropical, and gravity wave processes according to LF. Note that the vertical resolution requirements for the tropical domain and especially for gravity wave processes appear to be much more demanding than those for quasi-geostrophic flows.

According to LF for quasi-geostrophic flows the consistent combination of horizontal, ΔL, and vertical, ΔZ, scales is derived from the well known relationship:

$$\Delta L = \frac{N}{f_o} \Delta Z , \qquad (1)$$

where f_o is the characteristic Coriolis parameter, N is the Brunt-Vaiasala frequency.

For a regular spherical coordinate grid Table 1 (taken from LF) shows the approximately consistent horizontal and vertical resolution combinations for different latitudes.

It is worth mentioning that spatial resolution inconsistency is usually screened in atmospheric models by a rather strong spatial and/or temporal computational filtering applied to get rid of undesirable noise and/or to meet computational stability requirements. On the other hand, the substantial irregularity of conventional data distribution, and the use of satellite data swaths, usually only over the oceans for specific observation time windows, makes it difficult to trace the spatial and temporal resolution inconsistency for global observing systems.

This note is devoted to approximate experimental estimates of physically consistent horizontal and vertical resolution for atmospheric models and observing systems. When designing numerical experiments in order to show, directly and clearly, the effects of different model or observing system horizontal and vertical resolution combinations, we find that it is often difficult to separate the impact due exclusively to physical consistency of horizontal and vertical resolution from other virtually inevitable and mostly computational components of the performed calculations. In order to address the issue as straightforwardly as possible, we have taken some highly simplified approaches, and the obtained results should be considered as only approximate estimates of a spatial inconsistency signal we are trying to detect.

The results of numerical experiments with models having different horizontal and vertical resolutions are presented in Section 2. The experiments with observing systems are described in Section 3. Section 4 contains some concluding remarks. The PE baroclinic atmospheric model and analytical initial conditions are briefly described in the Appendix.

2. RESULTS OF NUMERICAL EXPERIMENTS WITH ATMOSPHERIC MODELS

The hypothesis we wish to verify is as follows: If the numerical approximation of model equations is accurate enough, and appropriate physically consistent requirements for vertical and horizontal resolution are fulfilled, the model should generate less noise than when such requirements are violated. If this hypothesis is correct, then estimated model lifetime (by which we mean the time needed for a model to break down) is a reasonable measure of model noise growth for different horizontal and vertical resolution combinations. We would like to know how model lifetime depends on resolution. The channel model and analytical initial conditions used for the experiments are briefly described in the Appendix.

Let us consider the results of numerical experiments with different model spatial resolution versions in terms of model life times. The different combinations of model horizontal and vertical resolutions are tested in the range of 50 km to 400 km in the horizontal, and from 0.375 km to 3.0 km in the vertical.

Simple analytical initial fields of a wave type superimposed on the constant zonal flow are used. Random noise in the range of ±20 m and ±2 m/s has been superimposed on initial height and wind fields respectively. Such an initial noise imitates an imbalance of initial conditions, and makes the model breakdown periods relatively shorter.

It is evident that the model will generate all scales (even those which are not present in initial conditions) eventually, and error growth in time depends on many different model properties and parameters quite apart from those pertaining to the numerical scheme used and its truncation errors. We have, however, attempted to constrain our experiments to show primarily the sensitivity of model generated noise to different combinations of horizontal and vertical resolution.

The model integrations continued until the potential temperature tendencies exceeded 300° K per hour which we took to unambiguously indicate a model break-down.

The results of the numerical experiments with the channel model are summarized in Table 2, where the lifetimes for different combinations of horizontal and vertical resolution are shown.

According to Table 2, the maximum life time period is obtained for the coarsest spatial resolution model version (ΔZ = 3 km, ΔS = 400 km). Starting from that model version, and increasing only horizontal or only vertical model resolution, results in a decrease of life time periods (see the first line and the first column of Table 2).

On the other hand, there are some specific combinations of horizontal and vertical model resolution, which lie on or near the diagonal of Table 2, which result in a relative increase of lifetimes . These particular combinations are: Δz = 3 km and ΔS = 400 km; Δz = 1.5 km and ΔS = 200 km; Δz = 0.75 km and ΔS = 200 km; Δz = 0.375 km and ΔS = 50 km. These optimal combinations correspond approximately to estimates of consistent resolution in LF (see Table 1). Other combinations generate more noise as manifested by reduced model lifetimes.

The above runs were repeated with a model modified by the introduction of very weak horizontal filtering in the form of a very high (32nd) order Shapiro filter (Shapiro 1970). This filters out only scales smaller than approximately 2-2.5 ΔS. Moreover, the filtering largely eliminates the initially superimposed random noise. Therefore, the model lifetimes are noticeably extended. Similarly, the effective horizontal resolution is decreased by the filter.

Nonetheless, model lifetimes presented in Table 3 are qualitatively similar to those of Table 2 in the sense that the consistent, or optimal combinations of horizontal and vertical resolution lie on or near the diagonal of the Table. Optimal resolution combinations are $\Delta Z = 3$ km and $\Delta S =$ 400-800 km; $\Delta Z = 1.5$ km and $\Delta S =$ 200-400 km; $\Delta Z = 0.75$ km and $\Delta S =$ 200-400 km; and $\Delta Z = 0.375$ km and $\Delta S = 100$ km. These optimal, or consistent combinations also correspond to theoretical estimates of Table 1.

The numerical experiments described above were performed with a specific channel model and analytical initial conditions. To see to what degree the conclusions derived are applicable to other models and initial data, we have looked at results obtained from runs with the adiabatic and diabatic versions of the 4th order GLA GCM (Kalnay, et al. 1983, Fox-Rabinovitz, et al. 1991) with no filters applied and with corresponding small time steps to avoid instability in polar domains. The real data initial conditions used are valid at 00Z 1 February 1979.

The model integration for each case continued until the surface pressure departed from the limits of 1000 mb ±300 mb; clearly the model results were no longer physically realistic. Therefore, reaching these limits is considered to be a measure of model lifetimes for these cases. Notice however, that the model integration could be formally continued. Note also that resolution combinations used are limited by model versions available.

The results of these adiabatic and diabatic model runs are presented in Table 4. Because we are using the global model (with the tropics included), real data as initial conditions with all resolvable scales included, not applying any filters, using a higher (4th) order numerical scheme, and more restrictive limits for surface pressures pointed out above, the model lifetime estimates of Table 4 are substantially shorter than those of Tables 2 and 3. However, the results obtained with the adiabatic version of this model also show that for the 4° x 5° horizontal resolution and the 2.2 km vertical resolution the model lifetime estimate is the largest among all combinations considered for the adiabiatic model, and the increase of the adiabatic model vertical resolution to 1.2 or 0.6 km leads to a substantial decrease of estimated model lifetime. This is true also for an increase of the horizontal adiabatic model resolution to 2° x 2.5°. At the same time, the increase of vertical adiabatic model resolution to 1.2 km for 2° x 2.5° horizontal resolution results in longer model lifetime, whereas the further increase of adiabatic model vertical resolution to 0.6 km for 2° x 2.5° horizontal resolution leads to decrease of model survival time. Therefore, for the case of adiabatic model only two among all considered combinations of horizontal and vertical resolution, namely, 4° x 5°, 2.2 km and 2° x 2.5°, 1.2 km, seem to be consistent (see Table 4). These results also correspond to the consistency requirements of LF.

We realize that the complete diabatic GCM, which includes besides dynamics the variety of parameterized physical processes (such as moist processes, turbulence, cloud-radiation interaction, and orographic effects), may impose additional requirements on consistent resolution combinations. Such a more complicated case does deserve a further detailed consideration but it goes well beyond the goal of this qualitative study.

However, we have performed experiments similar to those of adiabatic model with the full diabatic GLA GCM the results of which with available versions of the model are also presented in Table 4.

Note that on one hand, the full diabatic model may need finer vertical resolution to resolve, for example, moist processes but, on the other hand, the model turbulence works as strong physical dumping mechanism controlling noise development that does not take place for the adiabatic model. For 4° x 5° horizontal resolution versions of the diabatic model the increase of vertical resolution from 2.2 km to 1.2 km results in doubling the model lifetime whereas the further increase of vertical resolution to 0.6 km leads to the significant decrease of the model lifetime.

Therefore, the optimal, or consistent spatial resolution for these diabatic model runs is 4° x 5°, 1.2 km. For 2° x 2.5° horizontal resolution versions of the diabatic model the increase of vertical resolution results in the increase of model lifetimes. The most consistent combination of horizontal and vertical resolution for the diabatic model among three considered cases is 2° x 2.5°, 0.6 km. Therefore, the tentative conclusion from the experiments with the diabatic model is that finer vertical resolution is needed than for the adiabatic model with the same horizontal resolution.

The main conclusion of the experiments performed with both models is that when choosing or changing model spatial resolution the approximate estimates shown in LF may provide some guidance for achieving physically consistent combinations of horizontal and vertical model resolution.

3. NUMERICAL EXPERIMENTS WITH OBSERVING SYSTEMS

Another type of numerical experiment, concerning the problem of consistent horizontal and vertical resolution, has been performed for two observation networks, namely, for the satellite data, and for conventional data observing systems. Note that the satellite data is relatively poorly resolved in the vertical and much better resolved in the horizontal compared to conventional data. Therefore, we may expect that these two observing systems might reveal spatial resolution inconsistency in different ways.

The new substantially revised version of the GLA 4-D data assimilation procedure of an intermittent type uses the Optimum Interpolation (OI) objective analysis technique (Susskind and Pfaendtner, 1989). The data assimilation system was run for 10 days prior to the final analysis time which, therefore, included forty consecutive analysis and first guess (or 6 h forecast) calculations. The forecast model used within the data assimilation system is the 17 layer GLA GCM (Fox-Rabinovitz, et al., 1991). The data used for the 4-D data assimilation experiments and analysis results are available at all fourteen mandatory levels from 1000 mb to 20 mb. The data within satellite swaths is available with rather fine (proximately 100 km) horizontal resolution. The analysis system was run twice with 4° and 2° horizontal resolution to verify robustness of obtained results.

The design of the experiments to verify the spatial resolution consistency for the systems is as follows: For imitating different combinations of effective horizontal resolution with the given vertical resolution for both systems, horizontal filtering is used as a tool for changing effective horizontal resolution. Different strength spherical harmonic filters (Swarztrauber, 1979) have been applied to analysis fields. Namely, the smaller scales have been sequentially filtered out by applications of filters with different truncations (or spectral cut-offs) corresponding to a wide range of 2° to 32°.

The unfiltered as well as all filtered analysis fields for both runs with 4° and 2° horizontal resolution have been verified against all available conventional data, as the most reliable information, and RMS differences, or errors are calculated at observation locations over each continent, and over the oceans.

It is assumed that the consistent combination of a given observational vertical resolution and an adjusted (through different strength filtering) effective horizontal resolution would manifest itself in decreasing or at least not substantial increasing RMS analysis errors, compared to those of unfiltered fields.

In other words, the consistent, or optimal combination of vertical and horizontal resolution is associated with a minimum of the RMS error. This minimum may sometimes be rather flat, and then the consistent combinations correspond to some range of effective horizontal resolutions rather than to a particular one.

Figure 1 presents some examples of the dependence of RMS analysis errors on filtering strength (or equivalently on effective horizontal resolution) for both observing systems (for the run with 4° horizontal resolution). The RMS errors are normalized by those of corresponding unfiltered analysis fields. The response to filtering is different for the two observing systems. For example, for conventional data analysis over such a rich data region as North America no filtering is usually needed in the troposphere (Fig. 1a), whereas for satellite data analysis for the region filtering the scales smaller than 12° results in decreasing the RMS errors. Therefore, for this case, the effective horizontal resolution for conventional data is 4° (unfiltered fields). For satellite data it is 12° because RMS error is minimal for this effective horizontal resolution but it grows significantly when stronger filters are applied.

The results of all experiments we performed are summarized in Table 5 where for given vertical observational resolutions of satellite and conventional networks the consistent effective horizontal resolutions are presented for two thick layers (from 100 mb to 20 mb, and from 1000 mb to 150 mb), and for different regions (North America, Eurasia, and the oceans). Recall that for unfiltered fields the horizontal resolutions are 4° or 2° for two system runs performed.

The approximate observational vertical resolution estimates for satellite data of Table 5 have been derived from Susskind and Reuter (1985). According to these estimates, the vertical resolution is approximately 2 km in the lower troposphere, and 4 km in the upper troposphere and lower stratosphere (below 100 mb). In the rest of the stratosphere the vertical resolution of satellite data is markedly larger than 4 km.

The radiosonde data has finer vertical resolution of approximately 1.5 km in the lower troposphere, and 2 km in the upper troposphere and lower stratosphere. Above 100 mb the vertical resolution for the data is in the range of 2 km to 3.5 km, and coarser above. In general, the vertical resolution for the satellite data network is noticeably coarser than that of conventional data especially in the stratosphere.

The corresponding estimates of effective horizontal resolutions which are consistent with a given vertical resolution for the two observing systems, differ significantly.

For the lower layer from 1000 mb to 150 mb for all regions, the combinations of the 2° effective horizontal resolution for lower tropospheric levels and 4° for other levels of the layer and the 1.5 km to 2 km vertical resolution appeared to be optimal, or consistent for the conventional data analysis. For these cases, the unfiltered 2° or 4° analysis fields have minimal RMS errors (Table 5).

For satellite data analyses for the lower layer with 2 km to 4 km vertical resolution, the consistent effective horizontal resolution is coarser than that of conventional data, and varies for different regions in the range of 8° to 16°.

Qualitatively similar results have been obtained for both observing systems for the upper layer extending from 100 mb to 20 mb. Namely, for conventional data with 2 km to 3.5 km vertical resolution, the consistent effective horizontal resolution varies from 4° to 12° for different regions, which is coarser than for the lower layer. This reflects the relative smoothness of analyses for upper levels due to characteristic scales of the fields and to a gradual decrease with height of data availability and quality.

For satellite data with definitely more than 4 km vertical resolution for the layer, the consistent effective horizontal resolution varies from 12° to 24° for different regions, which is substantially coarser than that of conventional data.

Because of lack of vertical resolution for satellite data (especially in the upper layer) it may not be necessary or useful to keep increasing the already high horizontal resolution, until finer vertical resolution for the data is available. Therefore, the increase of vertical resolution for satellite data seems to be desirable to match a fine horizontal resolution of the data.

The results described above (Table 5) are fairly close for two analysis runs with different horizontal resolution, 4° and 2°. The only difference is that over North American and Eurasian continents with dense conventional networks the unfiltered conventional data analyses calculated with the 2° horizontal resolution seem to be more accurate for the lower tropospheric levels, or for 1000, 850 and sometimes 700 mb levels.

In practice both conventional and satellite data are used. According to obtained results, it may make sense to implement a two stage analysis procedure: namely, to calculate, for example, first an analysis using only satellite data, then smooth it in the horizontal and to proceed with calculating an analysis with only conventional data using the smoothed satellite data analysis as a first guess.

The obtained estimates of consistent vertical and horizontal resolution for both observing systems are again in approximate agreement with the theoretical estimates of LF (see Table 1).

4. CONCLUSIONS

This paper has examined the consequences of inconsistent horizontal and vertical resolution in both atmospheric models and observing systems by means of some highly simplified experiments.

An adiabatic PE baroclinic atmospheric model with analytical initial conditions, and cyclic boundary conditions (a channel model), and the adiabatic and diabatic versions of the GLA GCM are used for the model experiments. Suitably defined model lifetimes are compared for different horizontal and vertical model resolution combinations under the assumption that noisier models will have shorter lifetimes. Our aim was to see whether consistent resolution helped minimize model noise. For numerical experiments with the channel model, the forecasts with disturbed initial conditions (where random noise was superimposed) were used for comparisons of different model spatial resolution. Model lifetime, in these cases, referred essentially to the time it took a model run to "blow up". Such lifetimes are reasonable estimates of the forecast error developments in time which are associated primarily with model physical spatial resolution inconsistency.

The experiments with atmospheric models have shown that there exist some consistent combinations of horizontal and vertical resolution for which life time period estimates are relatively larger, or noise generated due to spatial resolution inconsistency is smaller (Table 4). These estimates also correspond approximately to those estimated in LF (Table 1).

Experiments were also performed in order to determine the implications of consistent resolution for observing systems. In these experiments we compared satellite and conventional data networks. Objective analyses of heights and winds using either satellite data alone or conventional data alone were calculated, and then different strength spherical harmonic filters were applied in order to change effective horizontal resolution. All analysis experiments were run twice with 4° and 2° horizontal resolution to verify the robustness of obtained results.

It is suggested that the consistent combination of a given observational vertical resolution and an adjusted (through different strength filtering) effective horizontal resolution would result in decreasing or at least not substantial increasing RMS analysis errors compared to those of unfiltered fields. Therefore, the consistent, or optimal vertical and horizontal resolution is associated with a minimum of a RMS error. The minimum may sometimes be rather flat, and then the consistent combinations correspond to some range of effective horizontal resolutions rather than to a particular one. In such cases, however, no evident advantage results from the finer resolutions.

The experiments with conventional and satellite data have resulted in substantially different consistent spatial resolution combinations (Table 5). Namely, for satellite data with relatively poorer vertical resolution the consistent effective horizontal resolution is coarser than that of conventional data.

The experiments with the observing systems have shown that an excessive horizontal resolution in combination with a relatively poor vertical resolution may result in larger analysis RMS errors compared to those of a network with more consistent spatial resolution. The increase of vertical resolution for satellite data to match a fine horizontal resolution of the data is desirable. The results are again in qualitative agreement with the estimates of LF (Table 1).

In brief, using consistent horizontal and vertical resolution for both atmospheric models and observing systems appears desirable for better representation of large scale atmospheric phenomena and processes, and is certainly more economical.

ACKNOWLEDGMENTS

The authors want to thank Mr. R. Govindaraju, Mr. M. Seablom, and Mr. D. Lamich for programming support, and Mrs. Q. Philpot for typing the manuscript. The research was supported by NASA grant 578-41-25-20 at the Goddard Space Flight Center, and by NASA Grant NAGW 525 and National Science Foundation Grant ATM 8520354 at the Massachusetts Institute of Technology.

REFERENCES

Arakawa, A. and V. R. Lamb, 1977: Computational design of the basic dynamical processes of the UCLA general circulation model. In Methods of Computational Physics, 17, Academic Press, New York, 173-265.

Brown, J. A. and K. Campana, 1978: An economical time-differencing system for numerical weather prediction, Mon. Wea. Rev., 106, 1125-1136.

Fox-Rabinovitz, M. A., 1974: On economical semi-implicit integration schemes for forecast equations. Meteorologiya i Gidrologiya, 11, 11-19.

Fox-Rabinovitz, M.S., H. M. Helfand, A. Hou, L. L. Takacs and A. Molod, 1991: Numerical experiments on forecasting, climate simulation and data assimilation with the new 17-layer GLA GCM, Proceedings of the 9th NWP Conference, 21-25 Oct., 1991, Denver, Colorado, p. 506-509.

Fritsch, J. M., E. L. Magziner and C. F. Chappel, 1980: Analytical initialization for three-dimensional numerical models. J. of Appl. Meteor., 7, 809-818.

Gadd, A. J., 1978: A split explicit integration scheme for numerical prediction. Quart. J. Roy. Met. Soc., 104, 569-582.

Kalnay, E., R. Balgovind, W. Chao, D. Edelman, J. Pfaendtner, L. Takacs and K. Takano, 1983: Documentation of the GLAS fourth order GCM. NASA Tech. Memo., 86064.

Lindzen, R. S. and M. S. Fox-Rabinovitz, 1989: Consistent vertical and horizontal resolution, Mon. Wea. Rev., 117, 2575-2583.

Mesinger, F. and A. Arakawa, 1976: Numerical methods used in atmospheric models. Vol. I, WMO/ICSU Joint Organizing Committee, GARP Publ. Series, No. 17, 64 pp.

Persson, P. O. G. and T. T. Warner, 1991: Model generation of spurious gravity waves due to inconsistency of the vertical and horizontal resolution. Mon. Wea. Rev., 119, 917-935.

Shapiro, R., 1970: Smoothing, filtering and boundary effects. Rev. Geophys. Space Phys., 8, 359-387.

Simmons, A. J., 1991: Development of a high resolution, semi-Lagrangian version of the ECMWF forecast model. Proceedings of the ECMWF Seminar on Numerical Methods in Atmospheric Models, 9-13 September, 1991, Vol. II, p. 281-324.

Susskind, J. and D. Reuter, 1985: Intercomparison of physical and statistical retrievals from simulated HIRS2 ana AMTS data. In Advances in Remote Sensing Retrieval Methods, (Eds. A. Deepak, H. E. Fleming and M. T. Chahine), A. Deepak Publishing, 641-662.

Susskind, J. and J. Pfaendtner, 1989: Impact of interactive physical retrievals on NWP. Proc. Joint ECMWF/EUMETSAT Working Group on the Use of Satellite Data in Operational NWP. ECMWF, Reading, England.

Swarztrauber, P. N., 1979: On the spectral approximation of discrete scalar and vector functions on the sphere. SIAM J. Num. Anal., 16, 6-26.

APPENDIX

1. A BRIEF DESCRIPTION OF THE CHANNEL MODEL AND NUMERICAL SCHEME

For the numerical experiments in the text the PE adiabatic baroclinic atmospheric model (with only surface friction included) in x, y, p-coordinate system, and with cyclic boundary conditions, and simple analytical initial data is used.

The calculation of analytical initial data for the numerical experiments is done following Fritsch et al. (1980), and is described below.

For the finite-difference approximation of the model equations the horizontal Arakawa's *C*-grid (Mesinger and Arakawa 1976; Arakawa and Lamb 1977), and a uniform vertical grid of Lorenz type (Lorenz 1960) was used. For the time integration the economical explicit scheme (Brown and Compana 1978; Fox-Rabinovitz 1974) was applied.

No space filters are applied but the time filter (Asselin 1972) is used to control the computational mode of the leapfrog scheme.

The time step, Δt, when using the economic explicit scheme for the model version with the horizontal increment Δs = 400 km is Δt = 16 min, and for other model versions with finer horizontal resolution is correspondingly smaller according to the CFL criterion. The horizontal integration domain is a square with the sides equal to 4000 km. In the vertical a uniform grid in ln p was used for all vertical model resolution versions.

To be able to perform these rather time consuming experiments with all model versions more efficiently, the split explicit integration scheme (Gadd 1978) was applied in combination with the economical explicit scheme.

The application of split explicit scheme allows using three times longer time steps for the horizontal advection subsystem. Finally, for the horizontal resolution with Δs = 400 km the time step for the adjustment subsystem is Δt = 16 min, and for the advection subsystem

$\Delta t = 48$ min. For other horizontal resolution model versions the time steps are correspondingly smaller.

2. CALCULATION OF ANALYTICAL INITIAL DATA

Analytical initial conditions at pressure levels are calculated following Fritsch et al. (1980). The analytical data of a wave type are superimposed on a constant zonal flow. The analytical data calculation consists of the following steps: 1) calculation of analytical heights for the 1000 mb level using the mean height for the level estimated from real data; 2) computation of real potential temperatures from real data geopotentials using the hydrostatic equation, and determining the real vertical mean temperature profile; 3) calculation of analytical temperature fields using the real mean temperature profile; 4) calculation of analytical geopotentials for all levels above 1000 mb from analytical potential temperatures by hydrostatic equation; and 5) calculation of analytical winds for all levels from analytical geopotentials using the geostrophic relationship.

Table 1 - Consistent Vertical and Horizontal Resolution Combinations

Horizontal Resolution (deg)	Vertical Resolution (km)		
	Local 60°	Local 45°	Local 22.5°
1	0.34	0.39	0.28
2	0.68	0.78	0.55
4	1.35	1.55	1.10
8	2.70	3.10	2.19
16	5.40	6.20	4.40

Table 2. Model life time estimates (in days) for different combinations of horizontal and vertical resolution

Vertical Resolution ΔZ, km	Horizontal Resolution, ΔS, km			
	400	200	100	50
3.0	17	11.5	8.5	6.5
1.5	9.5	12.5	8.5	7.5
0.75	7.0	15.0	9.5	10.5
0.375	6.0	8.5	8.5	13.5

Table 3 - Model life time estimates (in days) for different combinations of horizontal and vertical resolution, when applying very high (32nd) order Shapiro filter (which filters out $\approx (2-2.5)\,\Delta s$ scales).

Vertical Resolution ΔZ, km	Horizontal resolution, ΔS, km			
	400 (x 2 = 800)	200 (x 2 = 400)	100 (x 2 = 200)	50 (x 2 = 100)
3.0	29.0	24.5	15.5	11.5
1.5	13.5	19.0	18.0	9.5
0.75	8.0	16.5	13.0	12.0
0.375	7.5	9.5	12.5	15.5

Note: The approximate effective resolution after filtering was applied is shown in the parenthesis where factor of 2 corresponds to filtering scales smaller than 2DS that is an effective horizontal model resolution for the experiment.

Table 4 - Breaking down periods (in days) for the adiabatic and diabatic versions of the 4th order GLA GCM when no filters are applied.

Vertical Resolution, ΔZ, km	Horizontal Resolution, ΔS, degrees			
	4 x 5		2 x 2.5	
	Adiabatic	Diabatic	Adiabatic	Diabatic
2.2	3.00	2.5	2.0	1.00
1.2	2.00	5.0	2.5	1.5
0.6	0.6	1.0	1.0	2.5

Table 5 - Consistent or optimal combinations of a given observational vertical resolution and an effective (or adjusted through filtering) horizontal resolution for different layers and regions for both satellite and conventional observing systems.

Layer, in mb	Approximate observational vertical resolution, in km		Effective horizontal resolution, in degrees	
	Satellite data	Conventional data	Satellite data	Conventional data
		North America		
100-20	>4.0	2.0-3.5	16-24	4-12
1000-150	2.0-4.0	1.5-2.0	12	2*-4
		Eurasia		
100-20	>4.0	2.0-3.5	12-16	4-8
1000-150	2.0-4.0	1.5-2.0	8-12	2*-4
		The Oceans		
100-20	>4.0	2.0-3.5	12-16	4-12
1000-150	2.0-4.0	1.5-2.0	12-16	4

* For lower tropospheric levels (1000, 850, and sometimes 700 mb).

FIGURE CAPTION

Fig. 1. Relative RMS height analysis errors (normalized by the corresponding RMS error for unfiltered analysis fields valid at 00z February 10, 1979) as functions of effective horizontal resolution (obtained by an application of different strength filters) for the North American and the oceans regions and for 500 mb and 50 mb levels. The solid line is for the conventional data analysis, and the dashed line is for the satellite data analysis. The analyses for the case are calculated with 4° x 5° horizontal resolution.

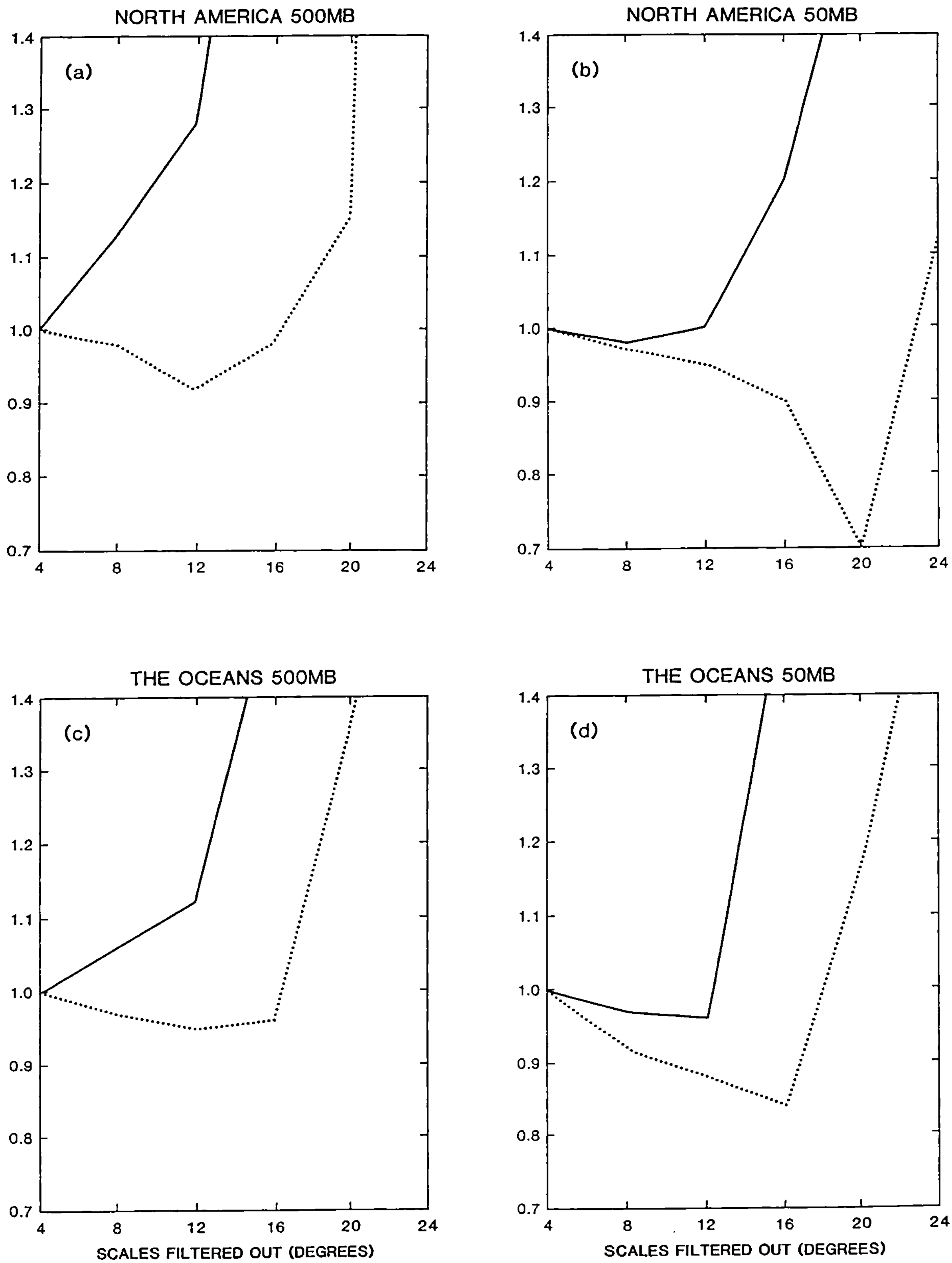

NORTH AMERICA 500MB
(a)
NORTH AMERICA 50MB
(b)
THE OCEANS 500MB
(c)
THE OCEANS 50MB
(d)
1.4
1.3
1.2
1.1
1.0
0.9
0.8
0.7
4
8
12
16
20
24
SCALES FILTERED OUT (DEGREES)